

---

---

STRUCTURE OF CHEMICAL  
COMPOUNDS. SPECTROSCOPY

---

---

## Structure of Water Clusters with Captured Methane Molecules

A. E. Galashev

*Institute of Industrial Ecology, Ural Branch, Russian Academy of Sciences, Yekaterinburg, Russia*

*e-mail: galashev@ecko.uran.ru*

Received September 9, 2013

**Abstract**—The adsorption of methane molecules by water clusters is studied by the molecular dynamics method. The structural changes that occur during the adsorption of methane are analyzed using the statistical geometry method, based on the construction of hybrid and simplified polyhedra. An enhancement in the ordering of the structure of the water cluster upon addition of methane molecules is revealed. This ordering manifests itself through an increase in the fractions of hydrogen hexagonal rings and linear pairs of hydrogen bonds.

**Keywords:** adsorption, water, cluster, methane, structure

**DOI:** 10.1134/S1990793114110049

### INTRODUCTION

The behavior of hydrophobic molecules of methane in bulk water has been studied in sufficient detail. Molecular dynamics studies showed that the concentration of methane has little effect on the structure of water and the formation of hydrogen bonds (H-bonds) between its molecules [1]. In particular, the number of H-bonds, their lengths, and angles are independent of the methane concentration. However, the number of hydrogen bonds and angles, as well as the self-diffusion coefficient of water, are temperature dependent. For example, an increase in temperature decreases the number of H-bonds and an increase in their bond angles. The structuring of the hydration shell of the water molecules was determined by the enhancements in the first and second peaks of the partial radial distribution function  $g(r_{O-O})$  at low temperatures.

In molecular dynamics based on first principles [2], the interatomic forces are determined directly from quantum-mechanical calculations. Simulation results obtained using this model, made it possible to study the dynamics of water molecules around hydrophobic solute molecules [3]. At certain distances from each other, stable water-molecule-built cells accommodating methane molecules were found. Such cells, similar to clathrate cavities, demonstrate how the solute molecule size can influence the local structure of water.

Water clusters can adsorb from the atmosphere a wide variety of molecules, including methane [4–7]. Hydrates cannot be formed under atmospheric conditions via the interaction of methane with water clusters, since relatively small water clusters ( $N < 100$ ) cannot have stable guest cells, with their structure being dissimilar to that of clathrates. In [4–6], only the spectral characteristics of aqueous cluster systems

with  $\text{CH}_4$  molecules were considered, whereas in [7], the structure of small water clusters ( $N = 10$ ), adsorbed methane molecules was examined.

The physicochemical properties of water clusters are largely determined by their structure. A hydrocarbon molecule attached to the cluster changes the original network of hydrogen bonds. With increasing number of adsorbed molecules, local changes in the H-bond network can become global. Structural analysis of small objects can be performed using the statistical geometry method [8], based on constructing Voronoi polyhedra (VP).

For a system with a limited number of degrees of freedom, VP can be constructed only for its inner part. However, even in this case, one should expect a strong change in the shape of the VP if the number of points that define the delimitation of the space is small. The manifestation of “boundary” effects, i.e., effects associated with a deficit of points at the periphery, makes VP significantly extended, while their volume increases dramatically. In the case of polyatomic molecules, atoms of one sort can serve as the centers of the polyhedra, whereas the nearest neighbors to them, forming the faces of the polyhedra, atoms of a different sort. For example, in the case of water, it is advantageous to use oxygen atoms as centers, whereas nearest neighbors should be hydrogen atoms. Such hybrid polyhedra (HP) are easier to build, since the number of hydrogen atoms is twice that of oxygen atoms. However, hybrid polyhedra are non-Voronoi polyhedra, since, when combined, do not fill tightly, all the space occupied by the molecules, without voids and overlappings. The faces of VP are built of cyclic formation of oxygen atoms, whereas the faces of HP, of rings of hydrogen atoms.

The aim of the present work is to study the structural characteristics of 50-molecule water clusters experiencing collisions with methane molecules, with the focus on changes in the hydrogen bonds in the clusters, the angular distribution of the hydrogen atoms with respect to the oxygen atoms, and the formation of  $m$ -mer hydrogen rings.

### SIMULATION MODEL

Molecular dynamics simulations were performed based on the DC-model of water [9], which was developed by refining the TIP4P rigid four-center model. The geometric parameters of the H<sub>2</sub>O molecule correspond to the experimental parameters of the water molecule in the gas phase:  $r_{\text{OH}} = 0.09572$  nm, the H–O–H bond angle is  $104.5^\circ$  [10]. The electric charges ( $q_{\text{H}} = 0.519e$ ,  $q_{\text{O}} = -1.038e$ ) are located at the centers of the H atoms and at point  $M$  on the bisector of the angle HOH at a distance of 0.0215 nm from the oxygen atom. The values of the charges and the position of point  $M$  were chosen so as to reproduce the experimental values of the dipole and quadrupole moments [11, 12], as well as the energy of the dimer and the characteristic distances in it predicted by ab initio calculations [13]. The tetrahedral structure is largely stabilized by a short-range Lennard-Jones interaction via oxygen atoms. Point  $M$  was singled out as the localization of the polarizability  $\alpha_i$  required to calculate the nonadditive polarization energy,

$$U_{\text{pol}}(\mathbf{R}_{1,\dots,N}) = -(1/2) \sum_i^N \mathbf{E}_i^0 \mathbf{d}_i^{\text{ind}}, \quad \mathbf{d}_i^{\text{ind}} = \alpha_i \mathbf{E}_i,$$

and the induced force acting on the molecule  $k$  [14],

$$\begin{aligned} f_k^{\text{ind}}(\mathbf{R}_{1,\dots,N}) &= -\nabla_k U_{\text{pol}} \\ &= \sum_{i=1}^N \mathbf{d}_i^{\text{ind}} (\nabla_k \mathbf{E}_i^0) + \sum_{i \neq k}^N \nabla_k (\mathbf{d}_i \mathbf{T}_k^{\text{ind}}), \end{aligned}$$

where  $\mathbf{R}_i$  is the radius-vector of point  $M$  in molecule  $i$ ;  $\mathbf{E}_i^0$  is the strength of the Coulomb field produced by the fixed partial charges, whereas  $\mathbf{E}_i$  is the field strength at the center of molecule  $i$  created by both the charges and the interaction of the induced dipole moments with these charges;  $\mathbf{d}_i^{\text{ind}}$  is the induced dipole moment of molecule  $i$ .

The dipole tensor is given by

$$\mathbf{T}_{ij} = \frac{1}{4\pi\epsilon_v} \frac{1}{r_{ij}^3} \left( \frac{3\mathbf{r}_{ij}\mathbf{r}_{ij}}{r_{ij}^2} - \mathbf{1} \right),$$

where  $\epsilon_v$  is the permittivity of free space.

The methane–methane interatomic interactions were described by the Mie–Lennard-Jones and Coulomb contributions:

$$\Phi_{ij}(r) = \epsilon_{ij} \left[ \left( \frac{r_0}{r_{ij}} \right)^{12} - 2 \left( \frac{r_0}{r_{ij}} \right)^6 \right] + \frac{q_i q_j}{r_{ij}}.$$

The values of the parameters  $\epsilon_{ij}$ ,  $r_0$ ,  $q_i$  for the H and C atoms belonging to the CH<sub>4</sub> molecule were taken to be 0.038 kcal/mol, 0.28525 nm, and 0.119e and 0.07382 kcal/mol, 0.43 nm, and  $-0.476e$ , respectively [15]. The parameters of the Lennard-Jones potential describing the methane–water interaction were calculated by the Berthelot–Lorentz formula:

$$\epsilon_{aw}^{(LJ)} = \sqrt{\epsilon_a^{(LJ)} \epsilon_w^{(LJ)}}, \quad \sigma_{aw}^{(LJ)} = \frac{\sigma_a^{(LJ)} + \sigma_w^{(LJ)}}{2},$$

where  $\epsilon_a^{(LJ)}$ ,  $\epsilon_w^{(LJ)}$  and  $\sigma_a^{(LJ)}$ ,  $\sigma_w^{(LJ)}$  are the energy and geometric parameters of the potential for the C and H atoms of the methane molecule and the O atom of the water molecule, respectively.

The methane molecule has the shape of a tetrahedron with the carbon atom at the center and the hydrogen atoms at the vertices. The H–C–H bond angle, the tetrahedral angle, is  $109^\circ$ . The distances between atoms in the CH<sub>4</sub> molecule are  $r_{\text{CH}} = 0.109$  nm,  $r_{\text{HH}} = 0.177$  nm. The CH<sub>4</sub> nonpolar molecule has a higher polarizability ( $2.6 \text{ \AA}^3$ ) than the water molecule ( $1.49 \text{ \AA}^3$ ) [16].

Models of flexible molecules were considered. The molecule was made flexible by using a procedure developed in the framework of the Hamilton dynamics [17–19]: the deformation of the molecule was produced by balancing the total potential force,

$$\mathbf{f}(\mathbf{u}) = -\frac{\partial \mathbf{r}}{\partial \mathbf{u}} \nabla \Phi(\mathbf{r}),$$

and the centrifugal force  $-\mu u \omega^2$ , where  $\mu$  is the reduced mass,  $u$  is the distance between the two atoms, and  $\omega$  is the vibrational frequency; the vector  $\mathbf{r}$  defines the point of application of the force.

The equations of motion of the molecules were solved by the fourth-order Gear's method [20]. The integration time step was  $2 \times 10^{-17}$  s. In a preliminary molecular dynamics calculation of duration  $2 \times 10^6 \Delta t$ , the  $T = 233$  K equilibrium state of a (H<sub>2</sub>O)<sub>50</sub> cluster containing no impurity molecules was prepared. The water cluster configuration at the time of 40 ps was subsequently used as the initial configuration for simulating the (CH<sub>4</sub>) <sub>$i$</sub> (H<sub>2</sub>O)<sub>50</sub> system ( $1 \leq i \leq 6$ ). Up to six methane molecules were added to the water cluster, by originally placing them in areas accessible for interatomic interactions. The attached CH<sub>4</sub> molecules were initially placed so that the smallest distance between the atoms in the methane molecule and the atoms of the water molecules was not less than 0.6 nm. The CH<sub>4</sub> molecule, placed at any of the axes passing through the center of mass of the (H<sub>2</sub>O)<sub>50</sub> cluster, had a random orientation. The cutoff radius for all the

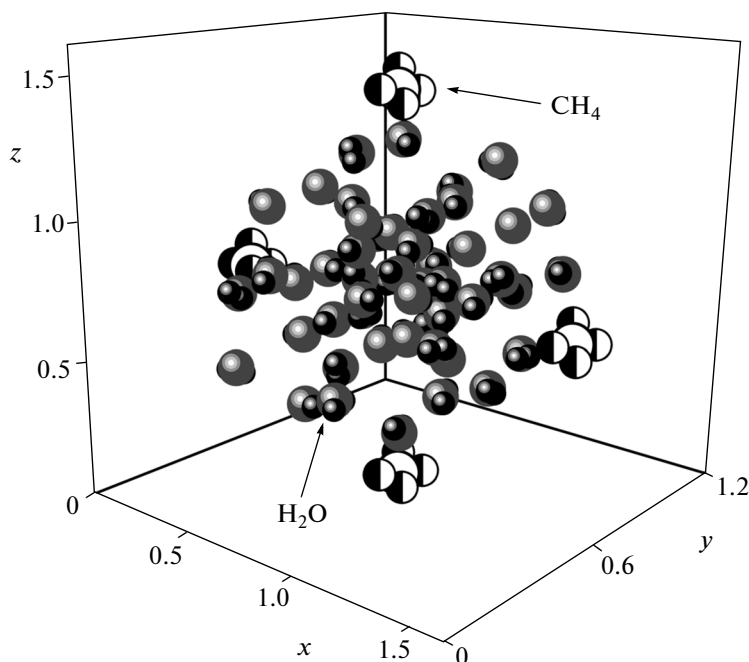


Fig. 1. Configuration of the  $(\text{CH}_4)_4(\text{H}_2\text{O})_{50}$  cluster at the time 50 ps. The coordinates of the molecules are given in nanometers.

interactions in the model was 0.9 nm. In the case where more than one  $\text{CH}_4$  molecule was added to the cluster of water, they were placed in pairs at the axes of a Cartesian coordinate system (but the couple could be incomplete). The coordinate axes were “filled” with  $\text{CH}_4$  molecules sequentially: for example, two methane molecules were placed on the same coordinate axis, but at the opposite sides of the center of mass of the cluster. The newly formed system was brought to equilibrium within a time interval of  $0.6 \times 10^6 \Delta t$ , and then, within a time interval of  $2.5 \times 10^6 \Delta t$ , the required physicochemical properties were calculated. The equations describing the translational and rotational motion of the molecules were solved using the scheme proposed by Sonnenschein [21]. This scheme is based on the Rodrigues–Hamilton parameters [22].

A detailed analysis of the structure of clusters was performed based on constructing hybrid polyhedra, which were built around 40 oxygen atoms that are closer to the center of mass of the cluster after thousand of time steps. The polyhedra were constructed around the oxygen atoms of water molecules, but the neighbors forming the faces could also be hydrogen atoms of the methane molecule. In constructing the HP, the hydrogen atoms belonging to the same  $\text{H}_2\text{O}$  molecule that contains the oxygen atom (center of the polyhedron) are excluded from the number of neighbors. To exclude small-scale thermal fluctuations, i.e., to deal with an averaged structure, sufficiently small faces of the polyhedra were excluded. This was achieved by removing edges with a length of  $l < 0.5\bar{l}$ , where  $\bar{l}$  is

the average edge length for the polyhedron. Using this procedure for constructing HP enables to in many cases to eliminate the double bonds of one molecule and the considered oxygen atom. Will be refer to polyhedra with excluded edges as simplified polyhedra (SP).

The smallest cluster of water, the water dimer, has a single hydrogen bond with an energy of  $(23 \pm 3)$  kJ/mol [23]. The distance  $r_{\text{OH}}$  between a covalently bonded H atom and the nearest-neighbor O atom that forms the hydrogen bond is 0.2 nm. For the H-bond, we used a range of  $r_{\text{OH}}$  distances similar to that reported in [24],  $0.15 \leq r_{\text{OH}} \leq 0.25$  nm. Most hydrogen bonds are not exactly linear ( $\angle\text{OHO} \sim 160^\circ\text{--}170^\circ$ ), with the distance  $r_{\text{OO}}$  between the neighboring oxygen atoms involved in the hydrogen bond is  $\sim 0.28$  nm [25]. In searching for hydrogen bonds, we also used an energy threshold for the H-bond of  $V_{\text{HB}} = 12.56$  kJ/mol [26].

## CALCULATION RESULTS

The adsorption of  $i$  methane molecules by the water cluster results in the formation of a  $(\text{CH}_4)_i(\text{H}_2\text{O})_{50}$  cluster. For example, Fig. 1 shows the configuration of the  $(\text{CH}_4)_4(\text{H}_2\text{O})_{50}$  cluster at the time of 50 ps. The methane molecules are arranged symmetrically relative to the center of the cluster in the vertical direction. Their orientation is rather arbitrary, being determined by the positions and orientations of the adjacent water molecules. Since the tetrahedral  $\text{CH}_4$  molecule carries outer positive charges (belonging to the H atoms), the vertex of the tetrahedron is located closer to the nega-

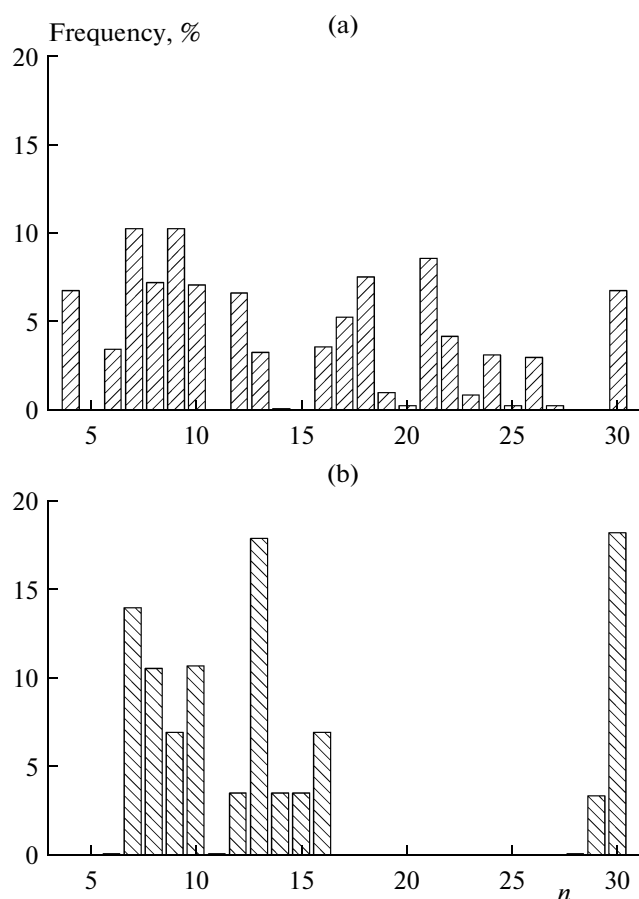


**Fig. 2.** Distribution of hybrid polyhedra over the number of face for the  $(\text{H}_2\text{O})_{50}$  cluster with (a) one and (b) six adsorbed  $\text{CH}_4$  molecules.

tively charged oxygen atom of the nearest-neighbor water molecule. There are also situations where hydrogen atoms of a methane molecule are located near the O atoms of two or even three  $\text{H}_2\text{O}$  molecules. A symmetrical arrangement of hydrophobic methane molecules causes a compaction of the water component of the cluster.

In the case of adsorption of a single methane molecule the distribution of HP over the number of faces ( $n$ -distribution) is represented by a wide variety of polyhedra, which, along with tetrahedra, includes tricontahedra (Fig. 2). The  $n$ -spectrum features a high proportion (~45%) of HP with low number of faces ( $n \leq 10$ ). Moreover, 7- and 9-hedra dominate the distribution. The fraction of these two amounts to 10.2%. Typically, HP with a small number of faces characterize the structure of the surface of the  $(\text{CH}_4)_i(\text{H}_2\text{O})_{50}$  cluster. The fraction of 4- and 30-hedra is 6.7%. The adsorption of six methane molecules substantially alters the  $n$ -spectrum of the cluster. The spectrum separates into two parts: with  $n \leq 16$  and  $n \geq 28$ . The first part of the spectrum is dominated by 13-hedra (17.9%), while the second, by 30-hedra (18.2%). Note also that the distribution of HP of the cluster with six

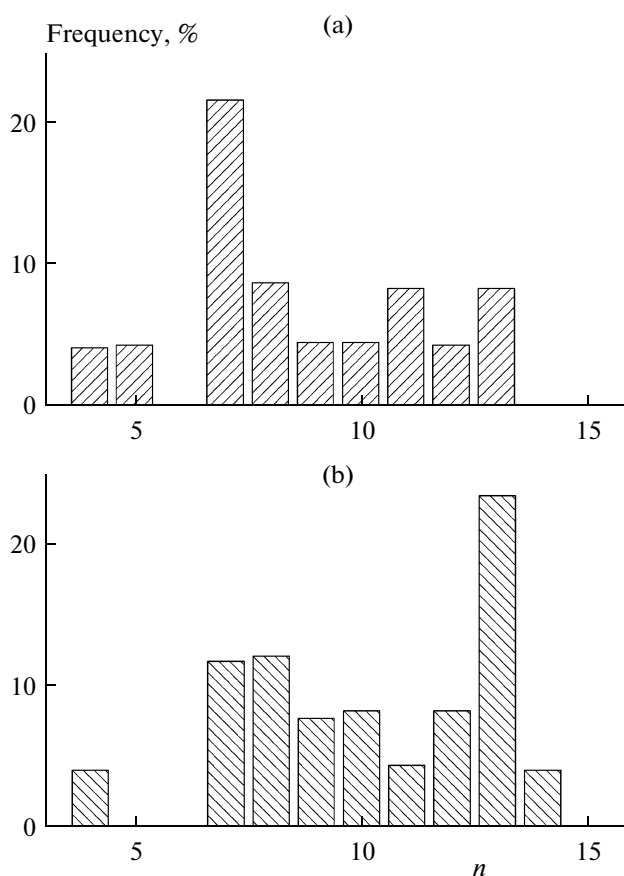


**Fig. 3.** Distribution of simplified polyhedra over the number of face for the  $(\text{H}_2\text{O})_{50}$  cluster with (a) one and (b) six adsorbed  $\text{CH}_4$  molecules.

adsorbed  $\text{CH}_4$  molecules has a high proportion of 7-hedra (14.0%). Hybrid polyhedra with a smaller number of faces (4- and 5-hedra) are absent in this spectrum. The fraction of 9-hedra is as low as 7.0%.

Exclusion of small faces leads to a significant change in the  $n$ -spectrum of polyhedra. For example, SP with number of faces of  $n > 13$  totally disappear at  $i = 1$ , whereas with  $n > 14$ , at  $i = 6$  (Fig. 3). The spectrum of SP of the water cluster with one adsorbed  $\text{CH}_4$  molecule is dominated by 7-hedra (21.6%), while that with six adsorbed  $\text{CH}_4$  molecules, 13-hedra (23.4%). At  $i = 6$ , the number of SP with seven faces decreases to 11.7%. In this case, the fraction of 4-hedra is low (4.1% at  $i = 1$  and 4.0% at  $i = 6$ ).

The distribution of HP faces over the number of edges ( $m$ -distribution) varies greatly upon adsorption of methane molecules on the water cluster. For example, the  $m$ -spectrum for  $i = 1$  stretches to  $m = 12$ , whereas for  $i = 6$ , only to  $m = 9$  (Fig. 4). In the first case, the maximum of the  $m$ -spectrum is localized at  $m = 4$ , whereas in the second, at  $m = 6$ . The fraction of quadrangular faces for  $i = 1$  is 26.8%, while that for  $i = 6$  is only 17.7%. The proportion of hexangular faces changes from 14.0% at  $i = 1$  to 32.9% at  $i = 6$ . The

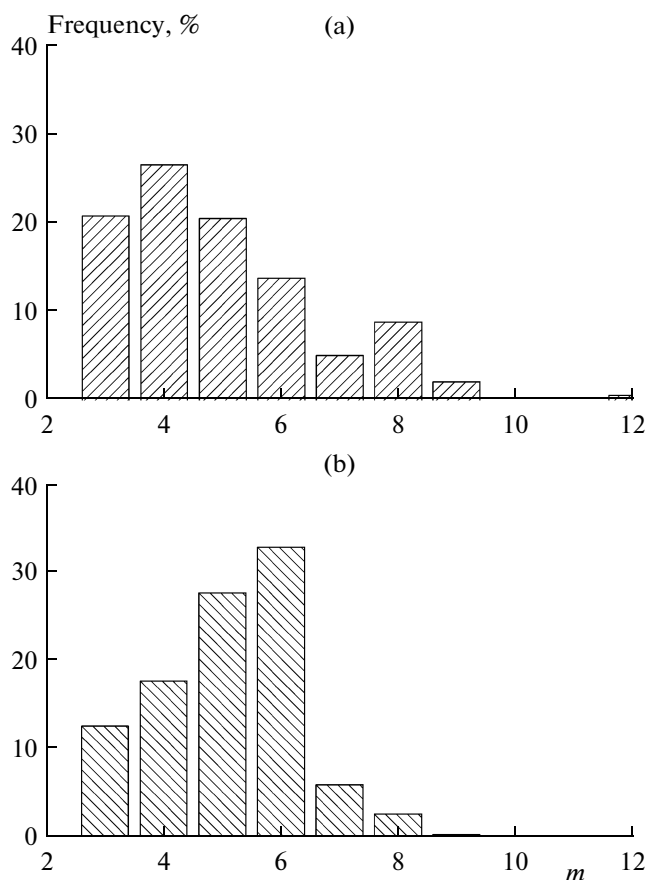


**Fig. 4.** Distribution of HP faces over the number face sides for the  $(\text{H}_2\text{O})_{50}$  cluster with (a) one and (b) six adsorbed  $\text{CH}_4$  molecules.

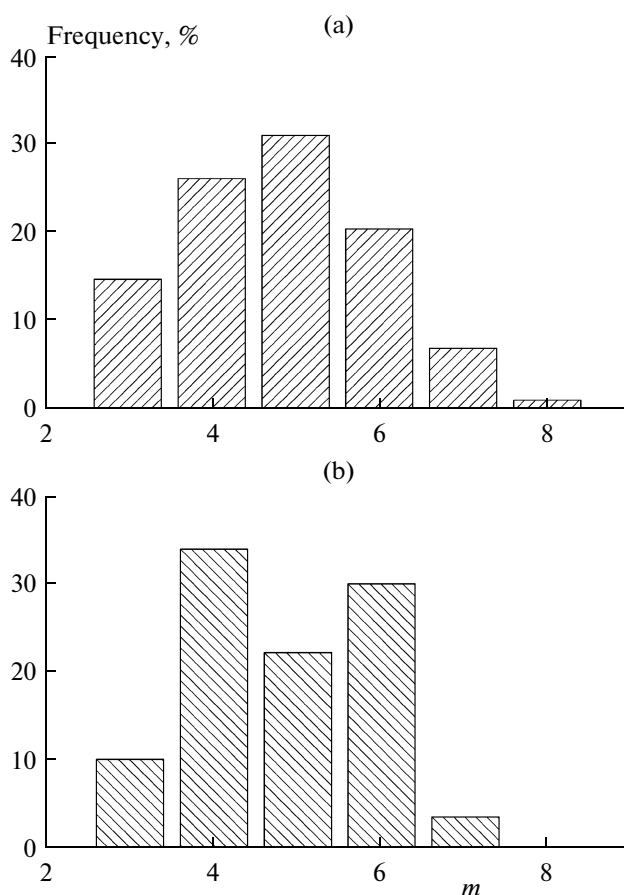


**Fig. 5.** Distribution of SP faces over the number face sides for the  $(\text{H}_2\text{O})_{50}$  cluster with (a) one and (b) six adsorbed  $\text{CH}_4$  molecules.

value of  $i = 1$  is characterized by a high proportion (21.0%) of triangular faces, while for  $i = 6$ , it decreases to 12.6%.

The changeover from HP to SP strongly transforms the  $m$ -distribution of polyhedra. When one methane molecule is added to the water cluster, the  $m$ -spectrum of SP terminates at  $m = 8$ , shifting to  $m = 7$  when 6  $\text{CH}_4$  molecules are added (Fig. 5). The maximum of the  $m$ -distribution is located at  $m = 5$  (30.9%) for  $i = 1$  and at  $m = 4$  (33.9%) for  $i = 6$ . In passing  $i = 1$  to  $i = 6$ , the fraction of triangular faces drops from 14.6 to 10.1%, while that of hexangular faces increased from 20.3 to 30.0%. The fraction of heptangular faces also decreases, from 6.9 to 3.6%.

In the case of adsorption of a single  $\text{CH}_4$  molecule, the range of excluded small faces is limited from above by  $m = 5$ , while for the adsorption of six methane molecules, this spectrum is cut off at  $m = 10$  (Fig. 6). For  $i = 1$ , the  $m$ -spectrum of small faces is dominated by quadrilaterals (69.3%), while the proportion of triangular faces is 28.4%. A similar spectrum for  $i = 6$  is dominated by triangular faces (57.2%), while the number of quadrangles reaches 19.0%.

The angular distribution of neighboring hydrogen atoms ( $\theta$ -distribution) near the oxygen center is shown in Fig. 7. The  $\theta$ -distribution features a large proportion of geometric neighbors creating an angle  $\theta$  within  $0^\circ \leq \theta \leq 15^\circ$ . For the adsorption of a single  $\text{CH}_4$  molecule by the water cluster, the fraction of such angles is 38.7%, reaching 54.4% when six methane molecules are added. The remainder of the  $\theta$ -distribution, with angles  $\theta > 15^\circ$  passes through a maximum at  $\theta = 72^\circ$  for  $i = 1$  and at  $\theta = 129^\circ$  for  $i = 6$ . The average angle of placement of adjacent H atoms relative to the O center is  $62.9^\circ$  for  $i = 1$  and  $50.2^\circ$  for  $i = 6$ . The distribution of “geometric” neighbors over the  $\angle\text{HOH}$  angle has the lowest intensity, 0.042% for  $i = 1$  and 0% for  $i = 6$ . In other words, the two parts of the  $\theta$  distributions (with  $\theta$  angles delimited by  $(30 \pm 3)^\circ$ ) are well resolved.

The dependence of the average number  $\langle n_b \rangle$  of hydrogen bonds on the number of  $\text{CH}_4$  molecules present in the cluster is displayed in Fig. 8. The value of  $\langle n_b \rangle$  varies nonmonotonically with increasing number  $i$ . The difference between the maximum (at  $i = 4$ )

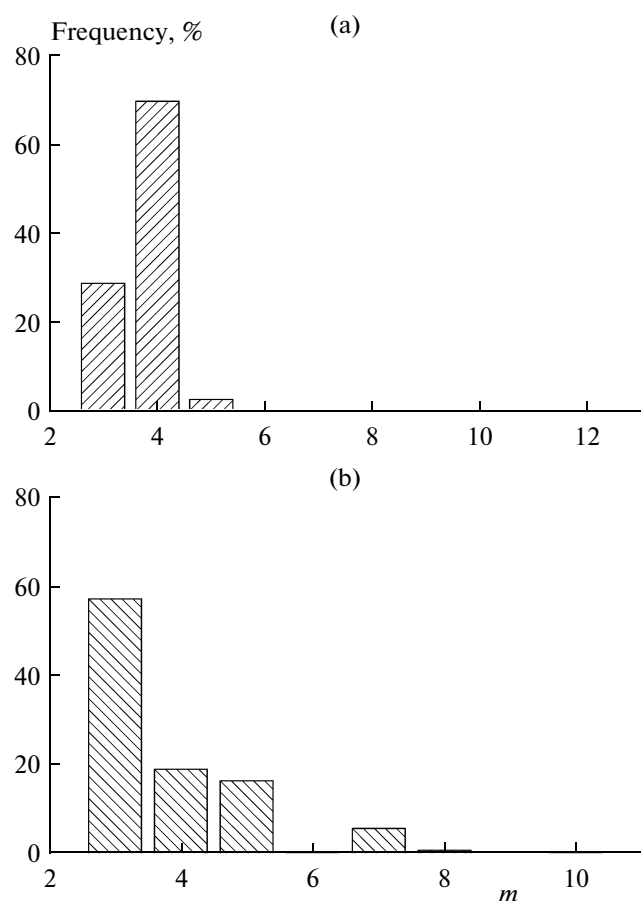


**Fig. 6.** Distribution of the small faces excluded during constructing the SP over the number of face sides for the  $(\text{H}_2\text{O})_{50}$  cluster with (a) one and (b) six adsorbed  $\text{CH}_4$  molecules.

and minimum ( $i = 5$ ) values of  $\langle n_b \rangle$  is 1.4. The value of  $\langle n_b \rangle$  averaged over six values of  $i$  is 3.7. That the value of  $\langle n_b \rangle$  for  $i = 4$  is highest is associated with a compaction of the water cluster, which is achieved at  $i \geq 4$  as a result of action of symmetrically in-plane arranged  $\text{CH}_4$  molecules. Placing fifth methane molecule to the water cluster at a position located outside the plane of the rest of the  $\text{CH}_4$  molecules leads to a loosening of the cluster and, as a result, to a sharp reduction in the number of hydrogen bonds. Adding sixth  $\text{CH}_4$  molecule symmetrically with respect to the fifth molecule, at the opposite side of the cluster, again caused a compaction of the water cluster. In this case, however, the value of  $\langle n_b \rangle$  does not reach that for  $i = 4$ .

In addition, the sequential adsorption of  $\text{CH}_4$  molecules causes significant changes in the H-bond length  $L_b$  distribution. While at  $i = 1$ , the  $L_b$ -spectrum features four groups of bands, with the most intense having a maximum at  $L_b = 0.245$  nm, for  $i = 6$ , the number groups reduces to three, the group with high intensity of the bands extends markedly, and the maximum of

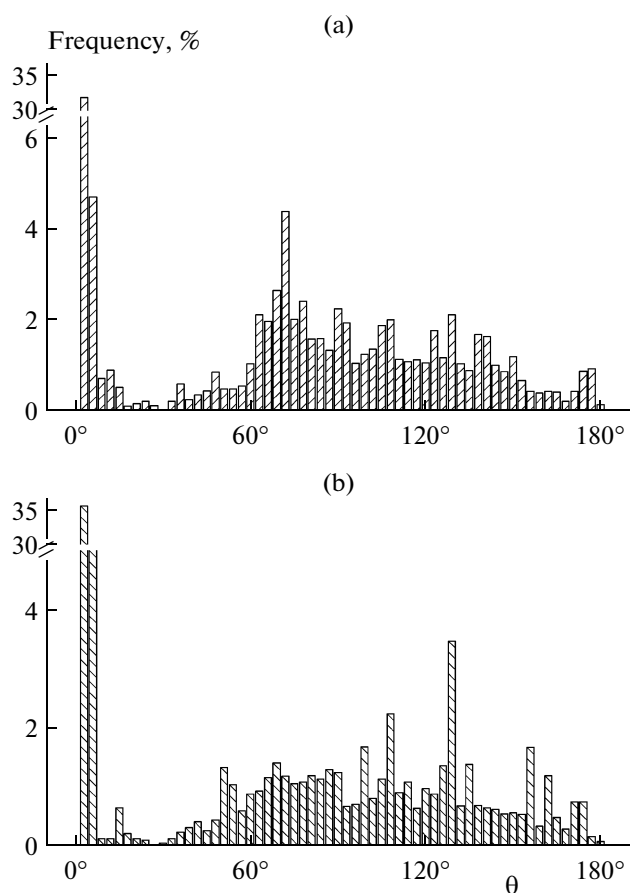


**Fig. 7.** Angular distribution of nearest geometric neighbors specified by hybrid polyhedra for the  $(\text{H}_2\text{O})_{50}$  cluster with (a) one and (b) six adsorbed  $\text{CH}_4$  molecules.

the  $L_b$  spectrum shifts to  $L_b = 0.230$  nm (Fig. 9). For  $i = 1$ , the maximum intensity of the band in the  $L_b$ -spectrum is 15.7%, while for  $i = 6$ , it reaches 23.8%. The average values of the H-bond length determined from the  $L_b$  spectrum for  $i = 1$  and  $i = 6$  are 0.218 and 0.210 nm, respectively.

## RESULTS AND DISCUSSION

In recent years, there has been significant progress in describing the properties of liquid water. Simulations have been performed for hundreds of models of force fields. However, despite great advances in computer technology, as well as in the development of ab initio molecular dynamics methods, it is still impossible to accurately calculate some of the properties of liquid water (for example, heat capacity, density, dielectric constant, compressibility) in a wide range of values. There is no satisfactory description of the molecular motion of the proton in the liquid. Not fully understood is the nature of the molecular surfaces of ice and liquid water. There are uncertainties in establishing the origin of anomalies in deep supercooling of

water. It is clear that the network of hydrogen bonds, in particular its vibrations and dynamics of rearrangement, determines the properties of the liquid. However, there are still no experimental studies that would provide more information on this at the molecular level. In addition, the reliability of the model of water for studying the solvation phenomena and biological processes often raises questions. The main obstacle to the solution of these problems lies in a correct description of the many-body system, or in the cooperative nature of the hydrogen bonds formed between water molecules. All the issues discussed are topical issues in studying the adsorption of methane by water clusters. Despite the hydrophobic nature of the interaction with methane, water clusters can adsorb a large number of  $\text{CH}_4$  molecules. Sequential addition of methane molecules to a water cluster changes the structure of the entire cluster. For example, when the structure of the cluster is presented in the form of simplified polyhedra, the switchover from the adsorption of one methane molecule to six molecules makes 13-hedra more abundant than 7-hedra. Upon addition of six  $\text{CH}_4$  molecules, the number of hexagonal faces in the SP increases by one-third compared to the  $i = 1$  case. The increase in the number of hydrogen hexagons is indicative of an increase in the ordering of the cluster and of its structure at  $i = 6$  becoming more similar to the structure of hexagonal ice. The transition from one to six adsorbed methane molecules is characterized by a significant increase in the number of small angles ( $\theta < 15^\circ$ ) in the mutual arrangement of neighboring H atoms relative to the O center, signifying that the number of linear pairs of hydrogen bonds increases.

Theoretical studies have shown that the formation of H-bonds is largely controlled by electrostatic interactions counterbalanced by electron exchange repulsion. However, dispersion also contributes significantly. Polarization is often a dominant factor in the many-body interaction. Data on polarization interactions derived from ab initio calculations are extremely difficult to accurately parameterize. In addition, ab initio molecular dynamics calculations based on the density functional method are limited to a relatively small size of the system (usually no more than 64 molecules). This can be a major obstacle for the development of quantitatively accurate general methods for testing and refining theoretical approaches. Recently, studies of the dynamics of the rupture of hydrogen bonds in water clusters began, with the results being compared to the predictions obtained within the framework of the mechanisms proposed to describe the dynamics of the bonding in liquid water [27].

The average lifetime of the hydrogen bond in liquid water is  $\sim 1$  ps. The time scales for a number of important dynamic processes in bulk water are comparable with this value. For example, the dielectric relaxation has two characteristic times:  $\sim 8$ – $9$  ps and  $\sim 1$  ps, so does the reorientation relaxation of the molecules:  $\sim 13$  ps and  $\sim 0.7$  ps, the proton mobility can be consid-

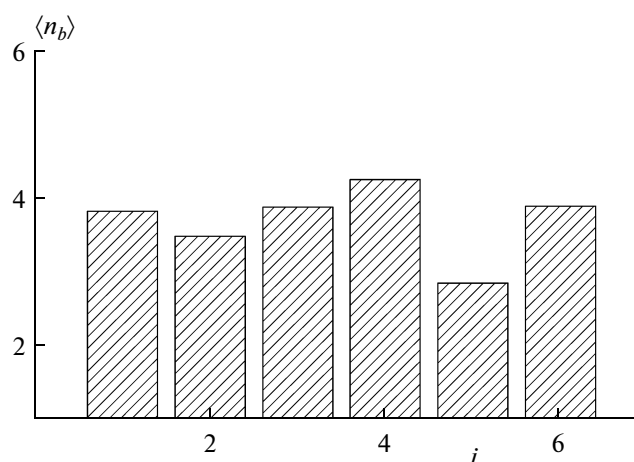


Fig. 8. Mean number of hydrogen bonds per  $\text{H}_2\text{O}$  molecule in the water clusters with  $i$  adsorbed  $\text{CH}_4$  molecules.

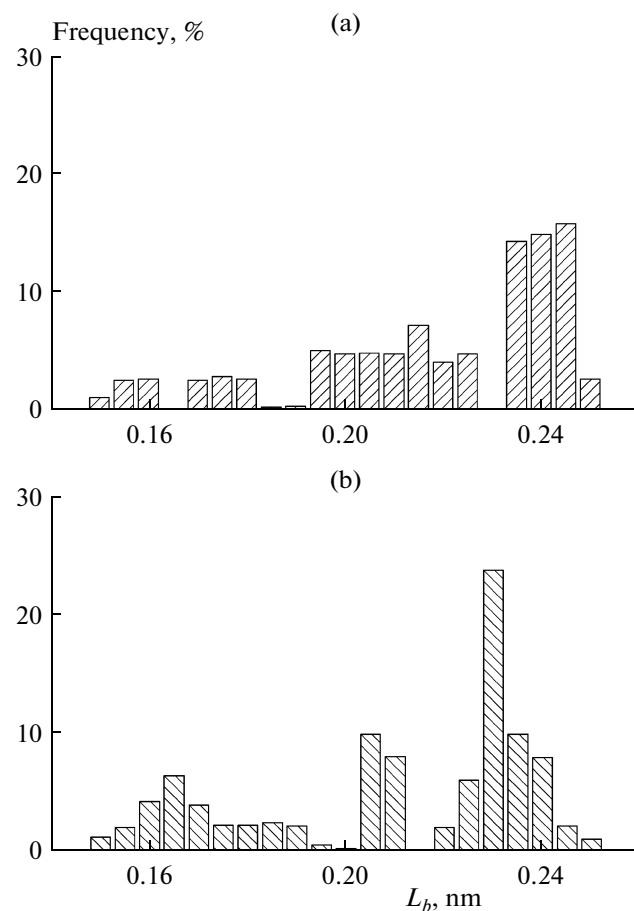


Fig. 9. Distribution of the length of the O–H hydrogen bonds for the  $(\text{H}_2\text{O})_{50}$  cluster with (a) one and (b) six adsorbed  $\text{CH}_4$  molecules.

ered for a time of  $\sim 1$  ps [27]. For clusters, as well as for liquid water, librations are a dominant means for rupture and formation of hydrogen bonds.

## CONCLUSIONS

The molecular dynamics method was used to study structural changes in water clusters with adsorbed methane molecules. The detailed structure of the clusters was investigated based on constructing hybrid and simplified polyhedra. For the cluster with six adsorbed CH<sub>4</sub> molecules, the distribution of HP over the number of faces is divided into two distinctly separated parts, with both the parts dominated by HP that were not prevalent for the cluster with one methane molecule. The pattern of the distribution of HP faces over the number of sides they have changes in passing from  $i = 1$  to  $i = 6$ . In the first case, the spectrum is dominated by quadrangles, whereas in the second, by hexagons. The spectrum for  $i = 6$  exhibits a sharp decrease at  $m > 6$ . Constructing simplified polyhedra is associated with excluding small faces of the HP, in particular quadrangular faces for  $i = 1$  and triangular for  $i = 6$ . The construction of SP revealed the transition to a more ordered structure in the water cluster with a large number of adsorbed methane molecules. This resulted in the formation of additional hydrogen hexagonal rings and pairs of linear hydrogen bonds. The latter may reflect the directions of placement of methane molecules in the cluster. With increasing the number of adsorbed methane molecules, the average length of O–H hydrogen bonds in the water cluster decreases.

## REFERENCES

1. J. Zhang, S. Piana, R. Freij-Ayoub, M. Rivero, and S. Choi, *Mol. Simul.* **32**, 1279 (2006).
2. R. Car and M. Parrinello, *Phys. Rev. Lett.* **55**, 2471 (1985).
3. J.-L. Li, R. Car, C. Tang, and N. S. Wingreen, *Proc. Natl. Acad. Sci. USA* **104**, 2626 (2007).
4. A. E. Galashev, V. N. Chukanov, A. N. Novruzov, and O. A. Novruzova, *High Temp.* **44**, 364 (2006).
5. V. N. Chukanov and A. E. Galashev, *Dokl. Phys. Chem.* **421**, 226 (2008).
6. A. E. Galashev, *Colloid. J.* **75**, 150 (2013).
7. A. E. Galashev, A. N. Novruzov, and O. A. Galasheva, *Khim. Fiz.* **25**, 26 (2006).
8. N. N. Medvedev, *Voronoi-Delaunay Method for Non-Crystalline Structures* (Sib. Otdel. RAN, Novosibirsk, 2000) [in Russian].
9. L. X. Dang and T.-M. Chang, *J. Chem. Phys.* **106**, 8149 (1997).
10. W. S. Benedict, N. Gailar, and E. K. Plyler, *J. Chem. Phys.* **24**, 1139 (1956).
11. S. Xantheas, *J. Chem. Phys.* **104**, 8821 (1996).
12. D. Feller and D. A. Dixon, *J. Phys. Chem.* **100**, 2993 (1996).
13. D. E. Smith and L. X. Dang, *J. Chem. Phys.* **100**, 3757 (1994).
14. P. Ahlstrom, A. Wallqvist, S. Engstrom, and B. Jonsson, *Mol. Phys.* **68**, 563 (1989).
15. M. H. New and B. J. Berne, *J. Am. Chem. Soc.* **117**, 7172 (1995).
16. *Chemists Manual*, Ed. by B. P. Nikol'skii (Khimiya, Leningrad, 1971), Vol. 1 [in Russian].
17. H. L. Lemberg and F. H. Stillinger, *J. Chem. Phys.* **62**, 1677 (1975).
18. A. Rahman, F. H. Stillinger, and H. L. Lemberg, *J. Chem. Phys.* **63**, 5223 (1975).
19. H. Saint-Martin, B. Hess, and H. J. C. Berendsen, *J. Chem. Phys.* **120**, 11133 (2004).
20. J. M. Haile, *Molecular Dynamics Simulation. Elementary Methods* (Wiley, New York, 1992).
21. R. Sonnenschein, *J. Comp. Phys.* **59**, 347 (1985).
22. V. N. Koshlyakov, *Problems in Dynamics of Solid Bodies and Applied Theory of Gyroscopes* (Nauka, Moscow, 1985) [in Russian].
23. R. N. Pribble and T. S. Zwier, *Science* **265**, 75 (1994).
24. G. A. Jeffrey and W. Saenger, *Hydrogen Bonding in Biological Structures* (Springer, New York, 1991).
25. S. Maheshwary, N. Patel, N. Sathyamurthy, A. D. Kul-karni, and S. R. Gadre, *J. Phys. Chem. A* **105**, 10525 (2001).
26. P. Mausbach, J. Schnitker, and A. Geiger, *J. Tech. Phys.* **28**, 67 (1987).
27. F. N. Keutsch and R. J. Saykally, *Proc. Natl. Acad. Sci. USA* **98**, 10533 (2001).

*Translated by V. Smirnov*